Clinics in Oncology

Research Article
Published: 01 Jul, 2023

A Comprehensive Study of *ROS1* Fusion in Patients with Non-Small-Cell Lung Cancer Using Novel *ROS1* Immunohistochemistry Clone (SP384)

*Wang Y[1,2], Wang Y[1,2], Jin Y[1,2], Cai X[1,2], Shen X[1,2], Zhou X[1,2] and Li Y[1,2]**

[1]Department of Pathology, Fudan University Shanghai Cancer Center, China

[2]Department of Oncology, Shanghai Medical College, Fudan University, China

Abstract

Background: The *ROS1* rearrangement is an important oncogenic target in lung cancer patients. Immunohistochemistry (IHC) is a commonly used method to identify potential *ROS1* rearrangement in routine clinical practice. In this study, we evaluated a novel *ROS1* immunohistochemistry clone (SP384) and investigated the correlation between different *ROS1* fusion variants and IHC staining features.

Methods: A total of 1380 lung cancers were screened by Next-Generation Sequencing (NGS) or Fluorescence *in situ* Hybridization (FISH) analysis for *ROS1* rearrangement prediction 37 *ROS1* NGS/FISH-positive and 173 *ROS1* NGS/FISH-negative NSCLC cases were selected for review in this study. All specimens were screened with a novel anti-*ROS1* IHC clone (SP384) from Ventana medical systems and a previous anti-*ROS1* IHC clone (D4D6) from Cell Signaling Technology. The IHC expression results were evaluated by two pathologists using H-score criteria. Next Generation Sequencing (NGS) is based on a targeted panel of 68 genes.

Results: A H-score of 150 or higher could be an optimal cut-off value for this novel anti-*ROS1* IHC clone (SP384) to discriminate *ROS1* rearranged cases with *ROS1* non-rearranged cases with 90% sensitivity and 99% specificity. Compared with anti-*ROS1* clone D4D6, SP384 has a higher sensitivity without compromising specificity. Different fusion partners have distinctive IHC staining features and several novel fusion alterations were found. CD74 is the most frequent occurring fusion partner with a strong and diffuse staining pattern. Two *ROS1* mutant cases in negative control group were also found presenting moderate, membranous staining with an H-score above 150.

Conclusion: The novel anti-*ROS1* IHC clone (SP384) could be an outstanding diagnostic alternative in routine clinical practice. Furthermore, this study highlights the importance of IHC in clinical practice that it can be a very supportive tool when used with molecular approaches to interpret fusion alterations like *ROS1* and help accurately predict the efficacy of targeted therapy.

Keywords: *ROS1*; Immunohistochemistry; Next-generation sequencing; Fusion partners; Functional outcomes; Targeted therapy

OPEN ACCESS

Correspondence:
Yuan LI, Department of Pathology, Fudan University Shanghai Cancer Center, Shanghai, 200032, China, Tel: +86-021-64175590

Received Date: *14 Jun 2023*
Accepted Date: *27 Jun 2023*
Published Date: *01 Jul 2023*

Citation:
Wang Y, Wang Y, Jin Y, Cai X, Shen X, Zhou X, et al. A Comprehensive Study of ROS1 Fusion in Patients with Non-Small-Cell Lung Cancer Using Novel ROS1 Immunohistochemistry Clone (SP384). Clin Oncol. 2023; 8: 2005.

ISSN: 2474-1663

Introduction

Lung cancer is one of the most common malignancies worldwide which accounts for over 2.21 million new cases and 1.80 million deaths in 2020, making it the leading cause of cancer death [1]. Non-Small Cell Lung Cancer (NSCLC) comprises roughly 85% of the lung cancer, usually present with a high rate of somatic mutation and gene rearrangement [2]. In the past years, tremendous advance has been achieved in the identification of druggable genetic alteration, such as mutant EGFR, mutant BRAF, rearrangement in ALK, RET, *ROS1* and etc. [3,4].

ROS1 rearrangement occurs in approximately 1% to 2% of the NSCLC and up to 3% of the lung adenocarcinoma [2,5]. With the development of molecular testing approaches like FISH and RNA/DNA based next generation sequencing, *ROS1* rearrangement gradually emerged as a relatively well-known oncogenic event in lung cancer patients [6,7]. Subsequently, targeted medicines like Crizotinib and Entrectinib were now reachable for patients who harbored *ROS1* fusions [8,9]. Since several studies have demonstrated appreciable clinical benefit and durable response of Crizotinib in patients with *ROS1* fusion, it's essential and demanding to accurately identify *ROS1* positive lung

cancer in routine clinical practice [9-11].

Immunochemistry (IHC) is widely used as a cost-effective and efficient method in cancer diagnosis and it's recommended as a screening test to identify *ROS1* rearrangement in patients with lung cancer [12-14]. To date, clinical use of anti-*ROS1* IHC antibody is limited to clone D4D6 [15], so in this study we evaluated a novel anti-*ROS1* antibody (SP384) to provide a diagnostic alternative.

A variety of fusion partners in *ROS1* rearrangement cases have been identified in previous studies like CD74, SDC4, EZR, GOPC and etc., [16-18]. However, few studies reported the IHC staining features of different fusion partners and whether it can contribute to the prediction of clinical effects in routine practice is still ambiguous. Here, we also use this novel anti-*ROS1* IHC antibody (SP384) to investigate the staining features of different fusion partners to help us further explore and distinguish *ROS1* alterations.

In this study, we gave out a comprehensive study of Chinese lung cancer patients with *ROS1* rearrangement, not limited to molecular characteristics, clinicopathological features and Crizotinib response, but also evaluated a novel anti-*ROS1* IHC antibody (SP384) as another diagnostic candidate. Besides, we investigated the correlation between different fusion partners and IHC performance to help explore the functional outcome of *ROS1* alterations.

Materials and Methods

Patients

A total of 1,380 lung cancers were screened by Next-Generation Sequencing (NGS) or Fluorescence *in situ* Hybridization (FISH) analysis for *ROS1* rearrangement in our institute from January 2016 to May 2021. *ROS1* rearrangements were identified in 37 NSCLC cases including 29 surgical resection cases and 8 small biopsies. These cases were selected for review in this study. In addition, 173 *ROS1* FISH-negative or NGS-negative cases were included as negative controls.

Next-generation sequencing

Genomic DNA was extracted from the FFPE tissue samples using the QIAamp DNA Mini Kit, and targeted deep sequencing of mutational hotspots was conducted using a capture-based targeted sequencing panel that included all exons of 68 genes, as described previously [37]. The sequencing panel included mutations of all exons of 65 genes: Including *AKT1*, *ALK*, *APC*, *ATM*, *AXL*, *BRAF*, *BRCA1*, *BRCA2*, *CCND1*, *CDK4*, *CDK6*, *CDKN2A*, *CTNNB1*, *DDR2*, *EGFR*, *ERBB2*, *ERBB3*, *ERBB4*, *ESR1*, *FGF19*, *FGF3*, *FGF4*, *FGFR1*, *FGFR2*, *FGFR3*, *FLT3*, *HRAS*, *IDH1*, *IDH2*, *IGF1R*, *JAK1*, *JAK2*, *KDR*, *KIT*, *KRAS*, *MAP2K1*, *MET*, *MTOR*, *MYC*, *NF1*, *NOTCH1*, *NRAS*, *NTRK1*, *NTRK2*, *NTRK3*, *PDGFRA*, *PIK3CA*, *PTCH1*, *PTEN*, *RAF1*, *RB1*, *RET*, *ROS1*, *SMAD4*, *SMO*, *STK11*, *TOP2A*, *TP53*, *TSC1*, *TSC2*, *AR*, *ARAF*, *BCL2L11*, *CD74*, and *NRG1*. Copy number gains are evaluated for the first 60 genes. Gene fusions are evaluated for another 7 genes (*ALK*, *RET*, *ROS1*, *CD74*, *FGFR3*, *NRG1*, and *NTRK1*). Moreover, 3 major polymorphic sites in drug metabolism genes (*CYP2D6*, *DPYD*, and *UGT1A1*) are also detected. Of all the genes, we mainly evaluated 12 genes, including 8 major driver genes (*EGFR*, *KRAS*, *BRAF*, *ALK*, *ROS1*, *MET*, *RET*, and *PIK3CA*) and suppressor genes (*TP53*, *STK11*, *Rb1*, and *NF1*).

Immunochemistry (IHC)

Anti-*ROS1* IHC analysis was performed on a Benchmark ULTRA staining instrument (Ventana Medical Systems). FFPE tumor tissues were sectioned at a thickness of 4 mm and stained with anti-*ROS1* clone: *ROS1* (SP384) rabbit monoclonal primary antibody, following the manufacturer's instructions. The slides were reviewed by two pathologists who were blinded to the NGS and FISH results. The interpretation of the slides was based on both intensity and H-score criteria. Intensity is based on the criterion as follows: 3+ means strong staining is clearly visible (2x or 4x objective), 2+ means moderate staining is visible (10x or 20x objective), 1+ means weak staining is visible (40x objective), 0 means no detectable staining or less than 10% of the tumor cells are in weak staining. H-score criteria is based on the percentages of cells stained with intensities of 0, 1+, 2+, 3+ as follows:

$$[1 \times (\%\ \text{cells}\ 1+) + 2 \times (\%\ \text{cells}\ 2+) + 3 \times (\%\ \text{cells}\ 3+)]$$

Fluorescence *in situ* hybridization (FISH)

Formalin-Fixed Paraffin-Embedded (FFPE) specimens were conducted for each patient. FISH was performed on 3 μm thick slides of FFPE with break apart FISH probes specific for *ROS1* (Vysis *ROS1* Break Apart FISH Probe, Abbott Molecular, Chicago, IL, USA) according to the manufacturer's instructions on ThermoBrite Elite (Leica, Richmond, CA, USA). The fluorescence signals were analyzed using an Olympus BX53 fluorescence microscope (Olympus, Tokyo, Japan). Images were captured using the BioView™ system (BioView Ltd., Tel Aviv, Israel). Scoring was performed by two independent pathologists. The rearrangement-positive cells were defined as those with split signals or isolated 3′ signals (*ROS1* probes were orange and green respectively), cells with intact fusion signals or isolated 5′ signals were defined as *ROS1* rearrangement-negative. At least 100 tumor cells were scored. The specimen was considered as *ROS1*-rearranged if the positive cells constituted ≥ 15% of the enumerated tumor cells [13].

Results

Clinicopathologic features and clinical data of 37 NSCLC patients with *ROS1* rearrangements

The clinicopathologic features of 37 NSCLC patients with *ROS1* rearrangements were summarized in Table 1. Briefly, the median age of these patients was 52.5 and 23/37 patients (62.6%) were female. Most of the patients have a tumor size less than 3 cm and they were at a late stage at initial diagnosis with distant metastasis. Thirty-three cases (89%) were adenocarcinoma and no squamous cell carcinoma was observed. Smoking history was available for 29/37 patients and the majority of them were never-smokers. PD-L1 expression data was also available for 21 patients and PD-L1 expression was observed in 13/21 (62%) patients.

At this point, clinical data were only available for 8/10 stage IV patients and Crizotinib was prescribed as first-line therapy in half of the cases (Table 1). Briefly, the overall response rate to Crizotinib was 50% and the disease control rate was 75%. Unfortunately, no conclusion could be achieved regarding the relationship between different fusion partners and drug response due to insufficient data.

Molecular characteristics of 21 patients with *ROS1* rearrangements

Comprehensive molecular characteristics of 21/37 patients were available and they were depicted in Figure 1. In all, high rates of somatic mutation and genomic rearrangement were observed in these patients. Other than *ROS1* rearrangements, 90% (19/21) of the patients harbored at least one somatic mutation. Specifically, recurrent alterations in key pathways and process were found in these 21 *ROS1* rearrangement cases: tumor suppressor TP53 mutations

Table 1: Clinical and histopathological features of patients with *ROS1* rearrangements.

Features	Patients with *ROS1* rearrangements (n=37, %)
Median age (Years)	52.5 (26-74)
Gender	
Male	14 (37.8)
Female	23 (62.6)
Tumor size (cm)	
≤ 3	26 (70.3)
5-Mar	8 (21.6)
7-May	2 (5.4)
≥ 7	1 (2.7)
Histology	
Adenocarcinoma	33 (89.2)
Squamous cell carcinoma	0 (0)
NSCLC-NOS	4 (10.8)
Stage	
I	13 (35.1)
II	4 (10.9)
III	10 (27)
IV	10 (27)
Smoking History	
Never-smoker	23 (62.2)
Ever-smoker	6 (16.2)
Unknown	8 (21.6)
PD-L1 expression level	
TPS <1%	8 (27.6)
TPS 1%-49%	7 (24.1)
TPS >50%	6 (20.7)
Unknown	6 (27.6)
Crizotinib treatment for IV stage patients (n=8)	
First-line	4 (50)
Not First-line	4 (50)
Response to Crizotinib	
Progressive disease (PD)	2 (25)
Stable disease (SD)	2 (25)
Partial response (PR)	4 (50)
Complete response (CR)	0 (0)

were enriched in 9/21 (33.3%) of the cases, NOTCH pathway was involved in 6/21(19%) of the cases and WNT pathway was involved in 2/21 (9.5%) of the cases. DNA repair process related genes were also found frequently mutated in these *ROS1* rearrangement cases including BRCA1 and BRCA2, which respectively occurred in 2/21 (9.5%) of the cases.

Co-mutations with other known driver oncogenes were found in 14.3% (3/21) of the *ROS1*-rearranged cases: *Erb-b2 Receptor Tyrosine Kinase 2* gene (*ERBB2*) missense mutation was found in two cases (9.5%) and EGFR mutation (exon 21 missense mutation) was found in one case, in which the fusion alteration is *ROS1*-LOC101927919 (R25: L intergenic), a gene-intergenic fusion.

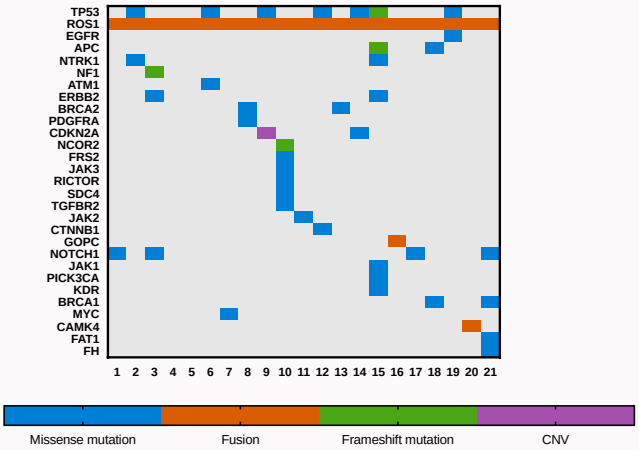

Figure 1: Comprehensive genetic profile of 21 patients with *ROS1* rearrangement.

ROS1 expression evaluated by both IHC clone SP384 and D4D6 using H-score method

The IHC results of *ROS1* expression were evaluated using the H-score method. H-score method is based on the percentages of cells stained with different intensities of 0, 1+, 2+ and 3+, ranging from 0 to 300. The distribution of H-score was interpreted in Figure 2A, 2B. When screened with SP384, the H-score of the *ROS1*-arranged cases largely ranged from 200 to 300 and most of the *ROS1* non-rearranged cases have no detectable staining except 17 cases, which have a highest H-score of 160. This result indicated that a H-score of 150 could be an optimal cut-off value for this novel anti-*ROS1* IHC antibody to discriminate *ROS1* rearranged cases with *ROS1* non-rearranged cases with 90% sensitivity and 99% specificity. As interpreted in Figure 2B, anti-*ROS1* IHC clone (D4D6) has 83% sensitivity and 99% specificity when 150 was used as a cut-off value. In comparison, SP384 has a higher sensitivity without compromising specificity.

The correlation between *ROS1* IHC expression and different fusion partners

Among these 37 *ROS1*-rearranged cases, data on different fusion partners were available for 29 cases. As shown in Figure 3A, the most frequent fusion partner is CD74 (n=16), followed by SDC4 (n=4) and EZR (n=3), other partners including SLC34A2, GOPC, and TPM3. In addition, a novel fusion partner: CD47 was revealed in our study and co-occurrence of two fusions (CD74-*ROS1*/CAMK4-*ROS1*) was also observed in this study.

The correlation between different fusion partners and IHC expression results was illustrated in Figure 3B. Considering the influence of tumor heterogeneity and quantification, only 21 samples with comparable tumor cells were selected for analysis and small biopsies were excluded. Most of the fusion partners had a H-score greater than 150. Remarkably, 9/21 cases were found showing strong, diffuse and homogenous immunoactivity with an H-score of 300. Among them, 55.6% of the cases were CD74-*ROS1* (5/9) (Figure 4A) while other fusions were SDC4-*ROS1* (3/9) and SLC34A2-*ROS1* (1/9). Novel CD47-*ROS1* fusion showed a weak, focal and granular staining pattern with a H-score of 100 (Figure 4B) and under the situation when CD74-*ROS1* fusion was accompanied by CAMK4-*ROS1* fusion, it showed moderate to strong, globular and heterogenous staining pattern with a H-score of 230 (Figure 4C). Besides, there's no detectable staining in LOC101927919-*ROS1* (L-intergenic: R25)

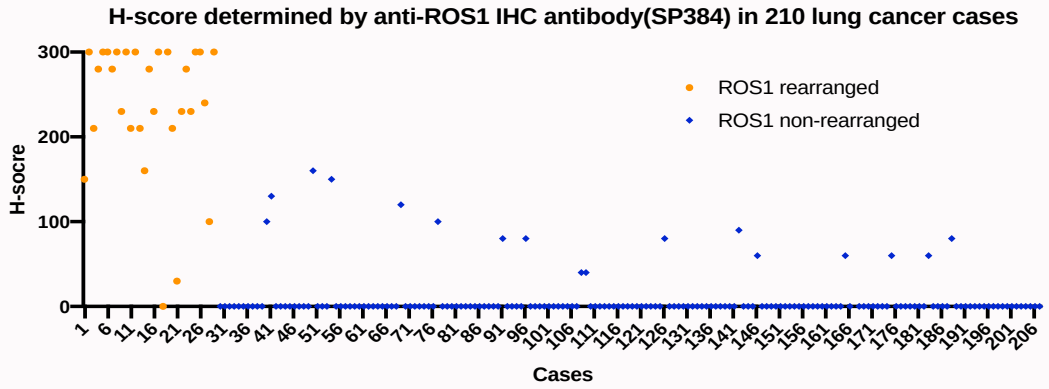

Figure 2A: The distribution of H-score in 210 lung cancer cases using novel anti-*ROS1* clone (SP384).

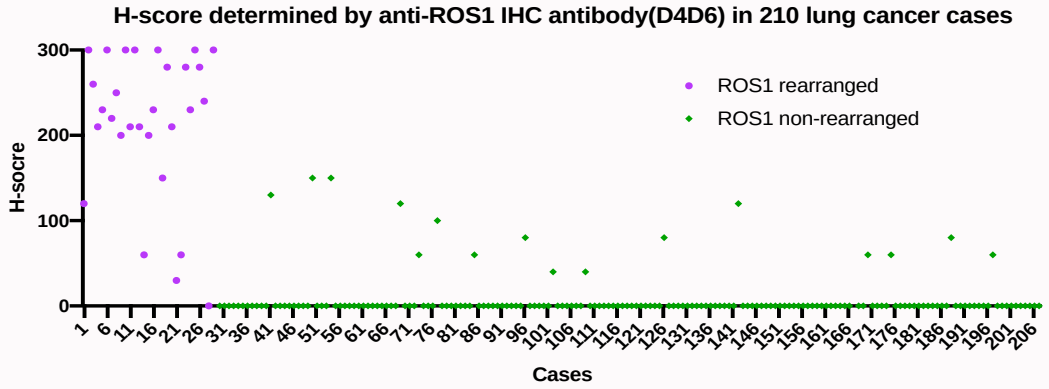

Figure 2B: The distribution of H-score in 210 lung cancer cases using previous anti-*ROS1* IHC clone (D4D6).

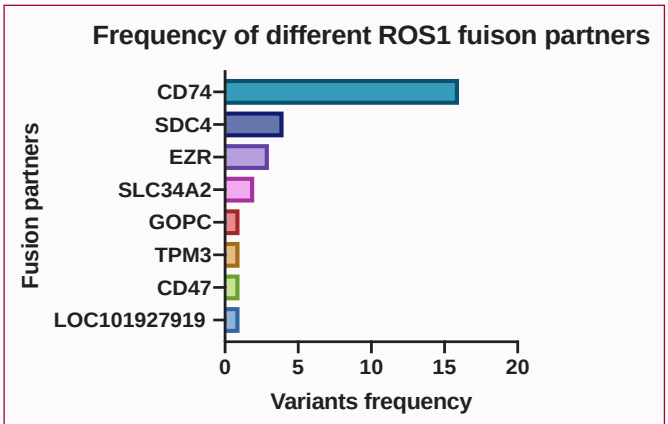

Figure 3A: Frequency of different fusion partners in 29 *ROS1* fusion cases.

fusion (Figure 4D). Representative IHC images of other fusion partners were shown in Figures 4E-4H.

ROS1 IHC staining observed in *ROS1* mutant cases and non-neoplastic cells

As interpreted in Figure 2, 17 *ROS1* fusion FISH/NGS negative cases were found showing anti-*ROS1* IHC expression and five cases had a H-score above 100. The NGS results of these five cases were available. Interestingly, 2/5 of the cases had a H-score above 150. These two cases both harbored *ROS1* mutations, which were missense mutations on exon 9 and exon 12, and they all presented as weak to moderate, heterogenous and membranous staining pattern on IHC (Figure 5A). The clinicopathological and comprehensive genetic profile of these two cases were shown in Figure 5B.

In addition, anti-*ROS1* IHC expression was also observed in some non-neoplastic cells, which presented as constant and moderate staining (Figure 5C). These cells usually presented as a cluster of cells located in the periphery of tumor nodule while not relevant to the histology of the tumor, indicating that they are reactive hyperplastic pneumocytes, most likely type II pneumocytes. They were found in both *ROS1* rearranged and non-rearranged cases.

Discussion

Regarding the fact that *ROS1* rearrangement only occurs in 1% to 2% of the lung cancer patients, few studies contain a large cohort of cases [19,20]. In this study, we give out comprehensive genetic profile, clinicopathological and clinical data of 37 *ROS1*-rearranged cases as well as the correlation between different fusion partners and IHC staining features to explore the potential functional outcome of *ROS1* alterations. Particularly, we use a novel anti-IHC clone (SP384) for the whole study and some conclusions have been drawn in our study. To the best of our knowledge, this is the first comprehensive study on *ROS1* fusion in Chinese NSCLC patients using this novel clone.

This study provides an overall evaluation on the novel anti-*ROS1* IHC antibody (SP384). In all, our study results shows that this newly developed anti-*ROS1* IHC clone could be an excellent screening tool in routine clinical practice. Regarding the diagnostic criteria, a H-score value of 150 or higher is an optimal cut-off value to accurately predict *ROS1* rearrangement with 90% sensitivity and 99% specificity. Compared with the clone D4D6, SP384 has a higher sensitivity

H-score Criterion	Intensity*	Fusion partners(Total n=21)
H-score =300	3	CD74-ROS1(C6:R33)
	3	SDC4-ROS1(S2:R33) n=2
	3	CD74-ROS1(C7:R32)
	3	SLC34A2-ROS1(S4:R32)
	3	CD74-ROS1(C6:R34)
	3	CD74-ROS1(C7:R34) n=2
	3	SDC4-ROS1(S4:R32)
H-score ≥ 150	3	CD74-ROS1 (C6:R34) n=5 *one case accompanied by CAMK4-ROS1(C12:R34)
	2	GOPC-ROS1(G4:R37)
	3	SDC4-ROS1 (S4:R32)
	3	TPM3-ROS1(Tintragenic:R35)
	3	EZR-ROS1(E10:R34) n=2
H-score 100-150	1	CD47-ROS1(C3:R34)
H-score <100	0	LOC101927919-ROS1(L-intergenic:R25)

* Intensity is based on the criterion as follows: 3+ means strong staining is clearly visible (2x or 4x objective), 2+ means moderate staining is visible (10x or 20x objective), 1+ means weak staining is visible (40x objective), 0 means no detectable staining or less than 10% of the tumor cells are in weak staining.

Figure 3B: Performance of novel anti-*ROS1* antibody (SP384) and its correlation with different *ROS1* fusion partners.
* Intensity is based on the criterion as follows: 3+ means strong staining is clearly visible (2x or 4x objective), 2+ means moderate staining is visible (10x or 20x objective), 1+ means weak staining is visible (40x objective), 0 means no detectable staining or less than 10% of the tumor cells are in weak staining.

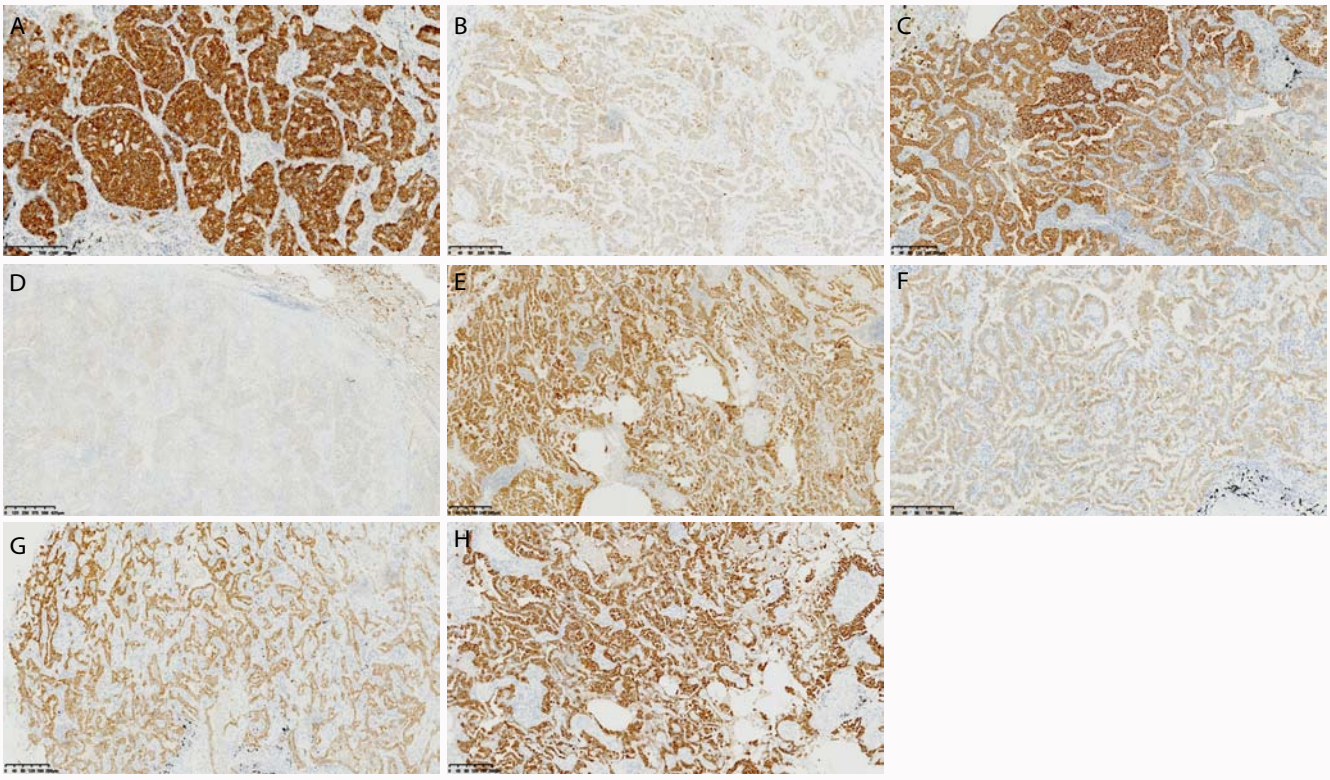

Figure 4A: Strong, diffuse, homogenous staining in CD74-*ROS1* fusion with an H-score of 300.
Figure 4B: Weak to moderate, focal, granular and heterogenous staining in novel CD47-*ROS1* (C3:R34) fusion with an H-score of 100.
Figure 4C: Moderate to strong, globular and heterogenous staining in a case when CD74-*ROS1* (C6:R34) fusion was accompanied by CAMK4-*ROS1* (C12:R34) fusion with an H-score of 230.
Figure 4D: No detectable staining in *ROS1*-LOC101927919 (R25: Lintergenic) fusion with an H-score of 0.
Figure 4E: Moderate to strong and granular cytoplasmic staining in EZER-*ROS1* (E10:R34) fusion with an H-score of 210.
Figure 4F: Weak to moderate, granular cytoplasmic staining in GOPC-*ROS1* (G4:R37) fusion with an H-score of 160.
Figure 4G: Moderate to strong, heterogenous and cytoplasmic staining in TPM3-*ROS1* (Tintragenic: R35) fusion with an H-score of 230.
Figure 4H: Strong, diffuse, homogenous staining in SLC34A2-*ROS1* (S4:R32) fusion with an H-score of 300.

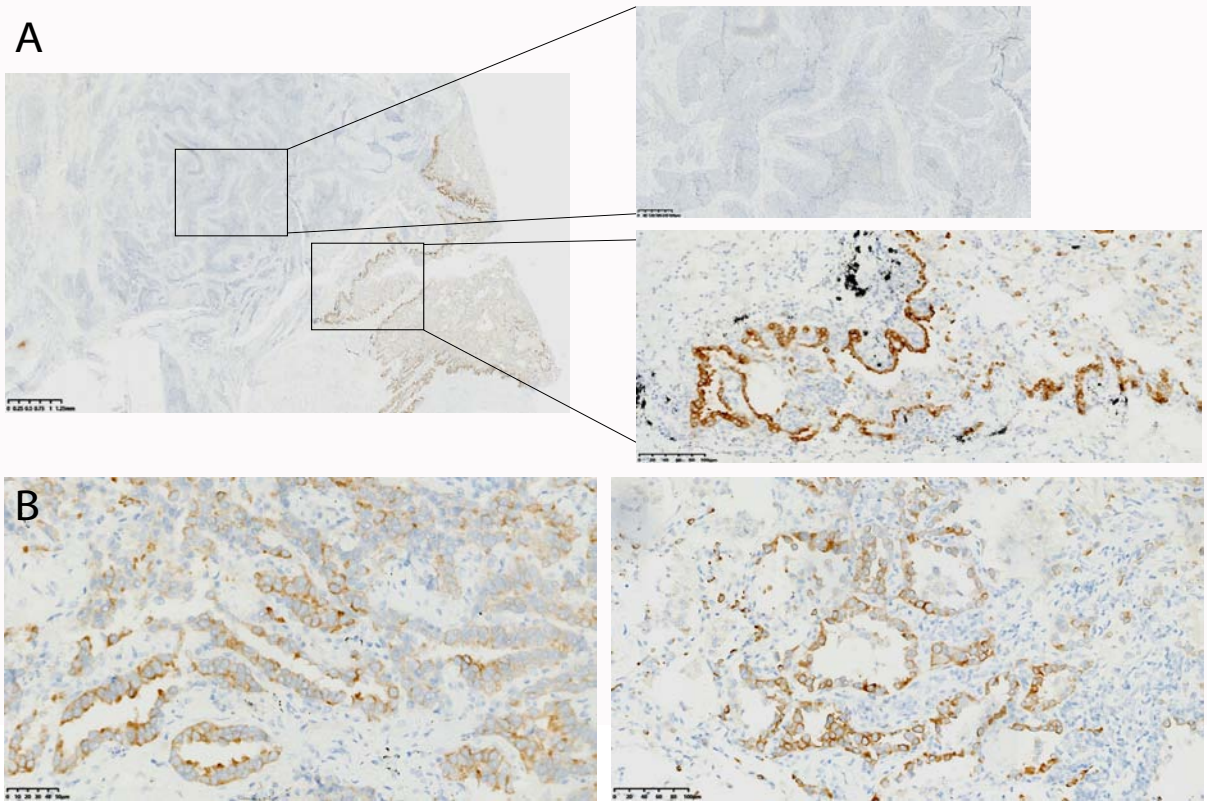

C

Age	Gender	Histology	Stage	IHC staining features	Molecular characteristics
53	Female	Adenocarcinoma	I	Moderate, membranous, heterogenous staining, H-score 160	ROS1 exon 9 missense mutation KRAS exon2 missense mutation BRCA1 exon17 missense mutation ATM exon13 splice site mutation ATM exon24 splice site mutation ERBB4 exon21 missense mutation APC exon16 missense mutation FGFR2 exon11 missense mutation RET exon4 frameshift mutation
38	Female	Adenocarcinoma	I	Moderate, focal, heterogenous staining, H-score 150	ROS1 exon 12 missense mutation ATM exon34 missense mutation

Figure 5A: Constant, moderate staining found in reactive type II pneumocytes located in the periphery of the tumor nodule.
Figure 5B: Moderate, membranous, heterogenous staining in two *ROS1* mutation cases with an H-score of 150 and 160.
Figure 5C: Clinicopathological features and molecular characteristics of two cases in control group which have a H-score above 150, showing moderate and heterogenous anti-*ROS1* IHC staining.

without compromising specificity. Besides, diffuse, moderate to strong staining pattern or a staining intensity 3+ is also supportive when used for *ROS1* arrangement prediction. One advantage of this novel clone (SP384) is that it usually presented as homogenous staining in *ROS1* positive cases, which could be useful when the samples are limited in size such as small biopsy or lymph node. This homogenous staining pattern was more frequently observed in the clone SP384 than clone D4D6.

As addressed in previous studies, our study also found that there's *ROS1* IHC staining in reactive type II pneumocytes [22]. These cells usually presented as a cluster located in the periphery of the tumors, showing constant, moderate staining pattern. Although the mechanism of this phenomenon is unclear, type II pneumocytes staining could be considered as internal positive control since it's not relevant to either the *ROS1* status or the histology of the tumors.

The occurrence of false-positive cases when using this novel antibody has been reported in two researches [22,23]. However, the molecular features of these cases are not available in those studies. In our study, we investigated all the false-positive cases which have an H-score higher than 100 and comprehensive molecular data were available. Notably, two cases were found harbored *ROS1* missense mutations, presenting as moderate, heterogenous and globular staining on IHC with a H-score above 150. *ROS1* mutation was reported associated with the drug resistance of Crizotinibin some *ROS1*-rearranged patients while the underlying mechanism has not been clarified [24,25]. Since IHC is a method of assessing protein level of gene expression, this finding in our study might provide some clues for further exploration on the role of *ROS1* mutation in the therapeutic outcome of targeted medicine.

Molecular diagnostic pathology plays an important role in routine

clinical work as it is helpful for the prediction of targeted medicine efficacy [26-28]. However, some challenges can be encountered for molecular approaches like DNA-based NGS when interpreting the fusion variants since it can only detect the genomic breakpoints but can't predict the functional outcome of these rearrangements [29]. A recent study published on journal of thoracic oncology showed that some ALK, *ROS1* fusions detected by DNA-based NGS actually exhibited poor response to Crizotinib and they were mostly uncommon fusion variants which were determined as protein-negative cases by IHC or RNA analysis [30].

In this study, we investigated the correlation between IHC staining features and different variants to further explore and distinguish fusion variants. Some findings are worth discussing here. Consistent with other studies, CD74 is the most frequent fusion variant which always present as a strong and diffuse staining pattern. It has been reported in several studies that patients with CD74-*ROS1* fusion who received Crizotinib as first-line therapy have a longer PFS than patients with non CD74-*ROS1* fusions [31,32], indicating that *ROS1* fusion variants which show strong and diffuse IHC staining with a high H-score have a greater chance to be functionally relevant and have a better response to targeted therapy like Crizotinib.

Besides, one DNA-NGS identified fusion variant was found showing no detectable staining. It is LOC101927919-*ROS1* (L-intergenic: R25), a gene-intergenic fusion. Since most of the well-known fusions are gene-gene fusions which thought to produce chimeric transcripts, it's controversial that whether gene-intergenic fusions can produce chimeric oncogenic mRNAs [33-36]. Considering the fact that there's no detectable IHC expression in this case, LOC101927919-*ROS1* (L-intergenic: R25) is more likely a functionally irrelevant *ROS1* alteration. In addition, one case harbored novel CD47-*ROS1* fusion was also found showing weak and focal staining with an H-score of 100, which should be determined as a protein-negative one based on the cut-off value of 150, indicating that this novel fusion has a higher possibility to be a functional irrelevant one. Unfortunately, analysis of clinical consequences on these *ROS1* fusion variants is still needed to draw definitive conclusions.

In summary, our results are consistent with the study reported by Esther et al. that this novel anti-*ROS1* IHC antibody (SP384) is an ideal diagnostic alternative in routine work [22]. More importantly, this study highlights the importance of IHC in clinical practice. It's not only a cost-effective and efficient method but it can also be very supportive when used with molecular approaches to interpret fusion alterations like *ROS1* and help accurately predict the efficacy of targeted medicine.

Author Contributions

Yuan Li designed this study and proofread the draft, provided substantive suggestions for revisions. Yichen Wang, Yan Jin, Xu Cai performed analysis and statistics, wrote the main manuscript. Xuxia Shen and Yue Wang collected the data and wrote partial sections of this draft. All authors have reviewed and approved the final manuscript.

Funding

This study was supported by National Nature Science Foundation of China (grant number 81972171) and CSCO-PILOT Cancer Research Foundation (Grant No. Y-2019AZMS-0492).

References

1. Sung H, Ferlay J, Siegel RL, Laversanne M, Soerjomataram I, Jemal A, et al. Global Cancer Statistics 2020: GLOBOCAN estimates of incidence and mortality worldwide for 36 cancers in 185 countries. CA Cancer J Clin. 2021;71(3):209-49.
2. Cancer Genome Atlas Research Network. Author Correction: Comprehensive molecular profiling of lung adenocarcinoma. Nature. 2014;511(7511):E12.
3. Pikor LA, Ramnarine VR, Lam S, Lam WL. Genetic alterations defining NSCLC subtypes and their therapeutic implications. Lung Cancer. 2013;82(2):179-89.
4. Yuan M, Huang LL, Chen JH, Wu J, Xu Q. The emerging treatment landscape of targeted therapy in non-small-cell lung cancer. Signal Transduct Target Ther. 2019;4:61.
5. Hirsch FR, Suda K, Wiens J, Bunn PA Jr. New and emerging targeted treatments in advanced non-small-cell lung cancer. Lancet. 2016;388(10048):1012-24.
6. Lin JJ, Ritterhouse LL, Ali SM, Bailey M, Schrock AB, Gainor JF, et al. *ROS1* fusions rarely overlap with other oncogenic drivers in non-small cell lung cancer. J Thorac Oncol. 2017;12(5):872-7.
7. Giustini NP, Bazhenova L. *ROS1*-rearranged non-small cell lung cancer. Thorac Surg Clin. 2020;30(2):147-56.
8. Drilon A, Siena S, Dziadziuszko R, Barlesi F, Krebs MG, Shaw AT, et al. Entrectinib in *ROS1* fusion-positive non-small-cell lung cancer: Integrated analysis of three phase 1-2 trials. Lancet Oncol. 2020;21(2):261-70.
9. Shaw AT, Ou SHI, Bang YJ, Camidge DR, Solomon BJ, Salgia R, et al. Crizotinib in *ROS1*-rearranged non-small-cell lung cancer. N Engl J Med. 2014;371(21):1963-71.
10. Shaw AT, Riely GJ, Bang YJ, Kim DW, Camidge DR, Solomon BJ, et al. Crizotinib in *ROS1*-rearranged advanced Non-Small-Cell Lung Cancer (NSCLC): Updated results, including overall survival, from PROFILE 1001. Ann Oncol. 2019;30(7):1121-6.
11. Wu YL, Yang JCH, Kim DW, Lu S, Zhou J, Seto T, et al. Phase II study of Crizotinib in east Asian patients with *ROS1*-positive advanced non-small-cell lung cancer. J Clin Oncol. 2018;36(14):1405-11.
12. Bubendorf L, Büttner R, Al-Dayel F, Dietel M, Elmberger G, Kerr K, et al. Testing for *ROS1* in non-small cell lung cancer: A review with recommendations. Virchows Arch. 2016;469(5):489-503.
13. Lindeman NI, Cagle PT, Aisner DL, Arcila ME, Beasley MB, Bernicker EH, et al. Updated molecular testing guideline for the selection of lung cancer patients for treatment with targeted tyrosine kinase inhibitors: Guideline from the college of American pathologists, the international association for the study of lung cancer, and the association for molecular pathology. Arch Pathol Lab Med. 2018;142(3):321-46.
14. Sholl LM, Sun H, Butaney M, Zhang C, Lee C, Jänne PA, et al. *ROS1* immunohistochemistry for detection of *ROS1*-rearranged lung adenocarcinomas. Am J Surg Pathol. 2013;37(9):1441-9.
15. Wang W, Cheng G, Zhang G, Song Z. Evaluation of a new diagnostic immunohistochemistry approach for *ROS1* rearrangement in non-small cell lung cancer. Lung Cancer. 2020;146:224-9.
16. Bergethon K, Shaw AT, Ou SHI, Katayama R, Lovly CM, McDonald NT, et al. *ROS1* rearrangements define a unique molecular class of lung cancers. J Clin Oncol. 2012;30(8):863-70.
17. Govindan R, Ding L, Griffith M, Subramanian J, Dees ND, Kanchi KL, et al. Genomic landscape of non-small cell lung cancer in smokers and never-smokers. Cell. 2012;150(6):1121-34.
18. Takeuchi K, Soda M, Togashi Y, Sakata S, Hatano S, et al. RET, *ROS1* and ALK fusions in lung cancer. Nat Med. 2012;18(3):378-81.

19. Lin JJ, Shaw AT. Recent advances in targeting *ROS1* in lung cancer. J Thorac Oncol. 2017;12(11):1611-25.

20. Park S, Ahn BC, Lim SW, Sun JM, Kim HR, Hong MH, et al. Characteristics and outcome of *ROS1*-positive non-small cell lung cancer patients in routine clinical practice. J Thorac Oncol. 2018;13(9):1373-82.

21. Yoshida A, Tsuta K, Wakai S, Arai Y, Asamura H, Shibata T, et al. Immunohistochemical detection of *ROS1* is useful for identifying *ROS1* rearrangements in lung cancers. Mod Pathol. 2014;27(5):711-20.

22. Conde E, Hernandez S, Martinez R, Angulo B, Castro JD, Collazo-Lorduy A, et al. Assessment of a new *ROS1* immunohistochemistry clone (SP384) for the identification of *ROS1* rearrangements in patients with non-small cell lung carcinoma: the ROSING study. J Thorac Oncol. 2019;14(12):2120-32.

23. Hofman V, Rouquette I, Long-Mira E, Piton N, Chamorey E, Heeke S, et al. Multicenter evaluation of a novel *ROS1* immunohistochemistry assay (SP384) for detection of *ROS1* rearrangements in a large cohort of lung adenocarcinoma patients. J Thorac Oncol. 2019;14(7):1204-12.

24. Sun H, Li Y, Tian S, Wang J, Hou T. P-loop conformation governed crizotinib resistance in G2032R-mutated *ROS1* tyrosine kinase: Clues from free energy landscape. PLoS Comput Biol. 2014;10(7):e1003729.

25. Katayama R, Gong B, Togashi N, Miyamoto M, Kiga M, Iwasaki S, et al. The new-generation selective *ROS1*/NTRK inhibitor DS-6051b overcomes crizotinib resistant *ROS1*-G2032R mutation in preclinical models. Nat Commun. 2019;10(1):3604.

26. Salk JJ, Schmitt MW, Loeb LA. Enhancing the accuracy of next-generation sequencing for detecting rare and subclonal mutations. Nat Rev Genet. 2018;19(5):269-85.

27. Gagan J, Allen EMV. Next-generation sequencing to guide cancer therapy. Genome Med. 2015;7(1):80.

28. Kruglyak KM, Lin E, Ong FS. Next-generation sequencing and applications to the diagnosis and treatment of lung cancer. Adv Exp Med Biol. 2016;890:123-36.

29. Rosenbaum JN, Bloom R, Forys JT, Hiken J, Armstrong JR, Branson J, et al. Genomic heterogeneity of ALK fusion breakpoints in non-small-cell lung cancer. Mod Pathol. 2018;31(5):791-808.

30. Li W, Guo L, Liu Y, Dong L, Yang L, Chen L, et al. Potential unreliability of uncommon ALK, *ROS1*, and RET genomic breakpoints in predicting the efficacy of targeted therapy in NSCLC. J Thorac Oncol. 2021;16(3):404-18.

31. Li Z, Shen L, Ding D, Huang J, Zhang J, Chen Z, et al. Efficacy of Crizotinib among different types of *ROS1* fusion partners in patients with *ROS1*-rearranged non-small cell lung cancer. J Thorac Oncol. 2018;13(7):987-95.

32. Xu H, Zhang Q, Liang L, Li J, Liu Z, Li W, et al. Crizotinib vs platinum-based chemotherapy as first-line treatment for advanced non-small cell lung cancer with different *ROS1* fusion variants. Cancer Med. 2020;9(10):3328-36.

33. Yun JW, Yang L, Park HY, Lee CW, Cha H, Shin HT, et al. Dysregulation of cancer genes by recurrent intergenic fusions. Genome Biol. 2020;21(1):166.

34. Zhang Y, Yang L, Kucherlapati M, Chen F, Hadjipanayis A, Pantazi A, et al. A pan-cancer compendium of genes deregulated by somatic genomic rearrangement across more than 1,400 cases. Cell Rep. 2018;24(2):515-27.

35. Mertens F, Johansson B, Fioretos T, Mitelman F. The emerging complexity of gene fusions in cancer. Nat Rev Cancer. 2015;15(6):371-81.

36. Li W, Liu Y, Li W, Chen L, Ying J. Intergenic breakpoints identified by DNA sequencing confound targetable kinase fusion detection in NSCLC. J Thorac Oncol. 2020;15(7):1223-31.

37. Wang Y, Xue Q, Zheng Q, Jin Y, Shen X, Yang M, et al. SMAD4 mutation correlates with poor prognosis in non-small cell lung cancer. Lab Invest. 2021;101(4):463-76.